

Analysis of Changes in NDVI Annual Cycle Models Caused by Forest Fire in Yangyang-gun, Gangwon-do Using Time Series of Landsat Images

Choi, Yoon Jo* · Cho, Han Jin** · Hong, Seung Hwan*** · Lee, Su Jin**** · Sohn, Hong Gyoo*****

Abstract

Sixty four percent of Korean territory consists of forest which is fragile for forest fire. However, it is difficult to detect the disaster-induced damages due to topographic complexity in mountainous areas and harsh weather conditions. For this reason, satellite imaging systems have been widely utilized to detect the damage caused by forest fire. In particular, ground vegetation condition can be estimated from multi-spectral satellite images and change detection technique has been used to detect forest fire damages. However, since Korea has clear four seasons, simple change detection technique has limitation. In this regard, this study applied the NDVI(normalized difference vegetation index) annual cycle modeling technique on time-series of Landsat images from 1991 to 2007 to analyze influence of forest fire of Yangyang-gun, Gangwon-do in 2005 on vegetation condition. The encouraging result was obtained when comparing the areas where forest fire occurs with non-damaged areas. The mean value of NDVI was decreased by 0.07 before and after the forest fire. On the other hand, annual variability of NDVI had been increasing and peak value of NDVI was stationary after the forest fire. It is interpreted that understory vegetation was seriously damaged from the forest fire occurred in 2005.

Keywords : Forest Fire, Landsat TM, NDVI, Annual Cycle Model

1. Introduction

Forest with high ratio of coniferous trees consists of 64 % of Korean territory and this property makes the land vulnerable to forest disaster(Byun, 2014). Yangyang-gun, Gangwon-do which has superiority of coniferous trees represents a vegetation characteristic of Korea. A damaged area from a forest fire which occurred in 2005 at Yangyang-gun was mostly comprised of pine forest(Kyosu newspaper, 2005). To prevent further damages over the area local authorities decided to plant deciduous trees which have fire-resistant properties. This decision gave the researcher an responsibilities to monitor the area using the state-of-art technology.

Generally there are two techniques used for monitoring vegetation; field surveying and remote sensing method. Field surveying can be an appropriate method to monitor the small details about the condition of vegetation but its application is limited when applying to the extensive areas and when obtaining time series data from the past. Remote sensing technique, on the other hand, is widely used to monitor the wide and inaccessible areas. It also provides useful information of the past if satellite imagery has been acquired periodically.

Landsat series, for example, first launched in 1972 have provided not only extensive coverage but also have extensively acquired many imagery over the same site. In addition with its capability to acquire

Received: 2016.05.27, revised: 2016.06.14, accepted: 2016.11.10

* Member, M. S. Student, School of Civil & Environment Engineering, Yonsei University, yoonjo15@yonsei.ac.kr

** Member, Staff, Korea Land and Geospatial Informatix Corporation, chj1221@lx.or.kr

*** Member, Ph. D. Student, School of Civil & Environmental Engineering, Yonsei University, hotaem@yonsei.ac.kr

**** M. S. Student, School of Civil & Environmental Engineering, Yonsei University, global_14@yonsei.ac.kr

***** Corresponding Author, Member, Professor, School of Civil & Environmental Engineering, Yonsei University, sohn1@yonsei.ac.kr

the imagery using multi-spectral bands, Landsat series have been widely used in the science community because the images are free to the general public since 2008.

Many studies related to the vegetation condition have been done in the field of drought monitoring, forest fire identification, agricultural productivity estimation, and vegetation regeneration monitoring (Labus et al., 2002; Peters et al., 2002; van Leeuwen, 2008; Vila et al., 2010). However, in most of these studies, vegetation conditions of a certain period have been represented by some indices in an individual satellite image. Accordingly, analysis of forest fire effect has been usually conducted based on the indices extracted from an individual image. However, since Korea has distinctive seasons, the characteristic of satellite imagery which has a periodicity is limited to analyze vegetation variability. To overcome these barriers, a technique which could reflect a continuity of vegetation cover is critical. Beck et al.(2006) developed a double logistic function model to describe NDVI(normalized difference vegetation index) time series in high-latitude environments. Verbesselt et al.(2010) presented a generic approach for detection and characterization of change in time series, which can robustly detect change. Jung et al. (2013) proposed harmonic model to characterize patterns of variation in MODIS NDVI time series data from 2006 to 2012. But when the change of data vary greatly it is difficult to apply this model.

Temperature is a primary factor affecting the rate of plant development(Hatfield and Prueger, 2015). Ha et al.(2007) also demonstrated that vegetation condition is closely related with average temperature. Bechtel(2012) proposed annual temperature cycle model which is approximated with a constant term plus sine function to characterize the annual cycle of land surface temperature with Landsat archives. Hong et al.(2015) applied annual temperature cycle model proposed by Bechtel(2012) to identify the variation of temperature inside the city. And they proved that the model fitted well in South Korea.

In this study, we extended the annual temperature cycle model to analyze vegetation variability before and after a forest fire. Yangyang-gun, Gangwon-do

was selected as an experiment site where big forest fire had frequently occurred since 1960(Lee et al., 2012). To analyze the influence of forest fire on the model parameters, nine AOIs(area of interest) were set as forest fire-affected area, area nearby the forest and mountainous area. To improve precision of the model, effects of clouds and cloud shadows were excluded by using Fmask(function of mask) algorithm and then outliers were removed by RIRLS-based(robust iteratively reweighted least squares) filtering technique. After investigating the NDVI trend using the NDVI annual cycle model, the seasonal changes of NDVI values using single Landsat images were analyzed and compared with the results of NDVI annual cycle modeling.

2. Study Site and Materials

2.1 Study Site

The study site locates in Yangyang-gun, Gangwon-do. A severe forest fire had occurred for 32 hours from April 4 to 6, 2005. Approximately 973 hectares of forest and Naksansa Temple were affected by the forest fire. Study area covers approximately $212,095,800m^2$ including both forest fire-affected area and non-affected area. Fig. 1 shows location of our study area and Fig. 2 shows the location of AOIs

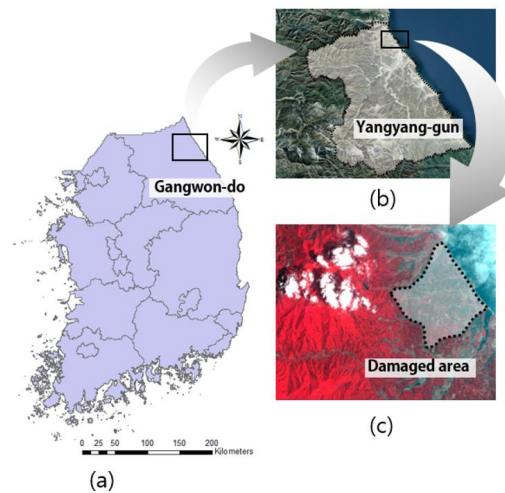


Figure 1. Location of study area: (a) Gangwon-do, (b) Yangyang-gun, (c) forest fire-damaged areas (2005/05/30)

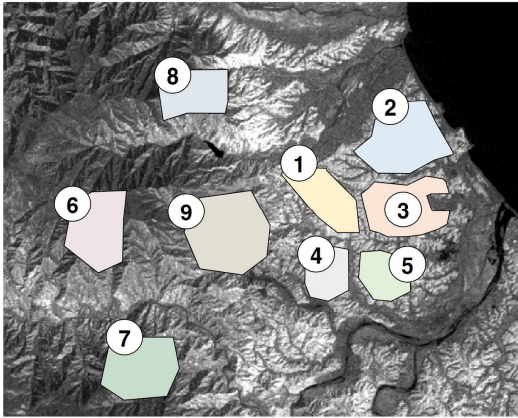


Figure 2. Location of AOIs

to identify the influence of forest fire on the NDVI annual cycle model.

In Fig. 2, the areas of 1, 2, and 3 indicate the areas affected by the forest fire, 4 and 5 the areas nearby the forest fire events, and 6, 7, 8, and 9 the mountainous areas, respectively.

2.2 Satellite Imagery

In this study, we used series of Landsat TM images. For maintaining consistency, Landsat ETM+ and OLI were not used in this study. Table 1 shows the numbers of Landsat TM scenes covering the study site. There were total 296 images available from 1991 to 2010. However, as shown in Table 1, the number of Landsat images after 2008 was not sufficient to apply the trend analysis of vegetation. Therefore, we performed the trend analysis only using 285 images obtained from 1991 to 2007 over the study areas.

Table 1. Number of Landsat TM images capturing Yangyang-gun, Gangwon-do from 1991 to 2010

year	No. of Image	year	No. of Image	year	No. of Image	year	No. of Image
1991	16	1996	16	2001	18	2006	21
1992	13	1997	16	2002	15	2007	15
1993	13	1998	18	2003	17	2008	1
1994	10	1999	18	2004	18	2009	5
1995	21	2000	21	2005	19	2010	5

3. Satellite Image Processing

3.1 Image Preprocessing

Since Landsat data are provided as DN(digital number) images with a range between 0 and 255, it is required to convert DN value into reflectance value(L_λ) when performing the land surface analysis. In this study, the algorithms proposed by Chander and Markham(2003) and NASA(2013) were applied to convert DN values into reflectance values. When multiple images are used, the effect caused by different solar zenith angles and the exoatmospheric solar irradiances can be compensated by converting original pixel values into reflectance(Chander and Markham, 2003). The formulas used for the conversion are listed in Eqs. (1) and (2).

$$L_\lambda = Gain \cdot DN + Bias \quad (1)$$

$$\rho_\lambda = \frac{\Pi \cdot L_\lambda \cdot d^2}{ESUN_\lambda \cdot \cos\theta_s} \quad (2)$$

where,

L_λ : radiance at the sensor's aperture
($W/(m^2 \cdot srad \cdot \mu m)$)

DN : original pixel value

$Gain$: gain value for a specific band

$Bias$: bias value for a specific band

ρ_λ : unitless planetary reflectance

d : Earth-Sun distance in astronomical units

$ESUN_\lambda$: mean solar exoatmospheric irradiance

θ_s : solar zenith angle

3.2 Noise Filtering

Since Landsat TM image typically includes cloud and cloud shadow pixels, they could make observation impossible and have an influence on the results of ground condition analysis. To release the influence of cloud and cloud shadow pixels, it is required to remove the cloud and cloud shadow pixels before the actual analysis. In this study, the noise filtering algorithm proposed by Zhu and Woodcock(2012) was applied. This algorithm can easily detect pixels of clouds and cloud shadows with high accuracy. The algorithm was conducted in two

steps. In its first step the object-based technique for classifying cloud and cloud shadow pixels is performed. The technique is called Fmask algorithm. Since the areas covered by clouds and cloud shadows present lower temperature than other areas, the shadow pixels can be extracted using the thermal infrared band information of Landsat image (Vermote and Saleous, 2007). After this, clouds and cloud shadows were matched based on the similarity of objects and sun angle.

Almost all cloud and cloud shadow pixels can be removed by Fmask, but some noise pixels might still remain. To remove the noise pixels and minimize the distortion caused by the noise pixels, RIRLS model was additionally adopted after performing the Fmask algorithm (Street et al., 1988; O'Leary, 1990; Zhu et al., 2012; Zhu and Woodcock, 2014). The pixels having lower or higher values than the matched value in the RIRLS model were filtered out by considering them as outliers. RIRLS model can be represented by Eq. (3).

$$\hat{\rho}(x)_{RIRLS} = a_0 + a_1 \cos\left(\frac{2\pi}{T}x\right) + b_1 \sin\left(\frac{2\pi}{T}x\right) + a_2 \cos\left(\frac{2\pi}{NT}x\right) + b_2 \sin\left(\frac{2\pi}{NT}x\right) \quad (3)$$

Where,

- x : Julian date
- T : number of days per year ($T=365$)
- N : number of years of Landsat data
- a_0 : coefficient for overall values for NDVI
- a_1, b_1 : coefficients for intra-annual change for NDVI
- a_2, b_2 : coefficients for inter-annual change for NDVI
- $\hat{\rho}(x)_{RIRLS}$: predicted value for the NDVI at Julian date x based on RIRLS fitting.

3.3 NDVI Calculation

The Landsat TM imagery consists of 7 spectral bands. From the multi-spectral imagery, the indices which represents ground condition can be computed with a combination of these bands. NDVI is the most powerful index to analyze the traits of vegetation.

The NDVI is computed by the reflectance values of the near infrared band (ρ_{NIR} ; band 4) and red band (ρ_{RED} ; band 3) on Landsat TM image. The formula to calculate NDVI is Eq. (4).

$$NDVI = \frac{\rho_{NIR} - \rho_{RED}}{\rho_{NIR} + \rho_{RED}} \quad (4)$$

3.4 NDVI Annual Cycle Model

Since ground vegetation condition generally follows annual variation trends, the methodology which can reflect continuity is required. Bechtel (2012) proposed annual temperature cycle model defined by sine function to characterize the annual cycle of land surface temperature with time series of Landsat images. To analyze the vegetation variability, this paper proposes annual NDVI cycle model applying annual temperature cycle model proposed by Bechtel (2012) using a time series of Landsat images. Annual cycle model is modelled with sine function and can be represented by Eq. (5).

$$f(d) = M + A \cdot \sin\left(\frac{2d\pi}{365.25} + \theta\right) \quad (5)$$

Where,

- $f(d)$: annual cycle model
- M : mean of NDVI
- A : amplitude of the annual NDVI cycle
- θ : optional phase shift from the equinox
- d : day of the cycle

M , A and θ of Eq. (5) were estimated by an unconstrained nonlinear optimization algorithm, which minimizes the square sum of the residuals (Bechtel, 2012).

4. Results

4.1 Noise Filtering

Fig. 3 shows Landsat TM image on May 14, 2005 and detected cloud and cloud shadow pixels in the image after applying the Fmask algorithm. As shown in Fig. 3(b), cloud and cloud shadow pixels were extracted.

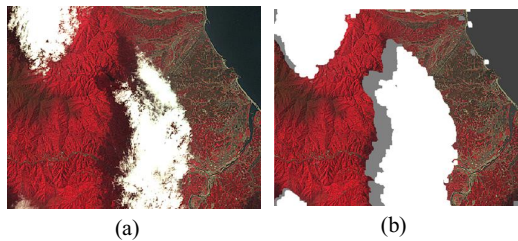


Figure 3. Results of applying Fmask: (a) Landsat imagery (2005/5/14), (b) cloud and cloud shadow pixels extracted from Landsat imagery by Fmask (white: cloud, gray: cloud shadow)

In order to create a stable annual cycle model, the remained noise pixels after applying Fmask were filtered out by RIRLS model. Forest fire caused significant changes on the vegetation conditions. For this reason, NDVI annual cycle modeling was conducted separately before and after on April 4, 2005, the day when a huge forest fire occurred.

Table 2 summarized the number of available images in each of the AOI after applying Fmask algorithm and RIRLS-based filtering technique. As shown in Table 2, about 97~116 scenes in each AOI after filtering were available among total 285 Landsat images. In other words, 59~66% of total images we used were filtered out in the final stage.

Table 2. Results of Fmask and RIRLS filtering

	Number of images		
	Before filtering	After Fmask filtering	After RIRLS filtering
AOI #1	285	147	107
AOI #2		156	116
AOI #3		152	115
AOI #4		146	99
AOI #5		147	108
AOI #6		140	97
AOI #7		153	108
AOI #8		148	107
AOI #9		149	105

4.2 NDVI Annual Cycle Models

From the Landsat images of which pixels of cloud and cloud shadow were removed, NDVI annual cycle model of each AOI were calculated. Fig. 4 shows the results of the annual cycle modeling. As shown in Fig. 4, the seasonal variation of NDVI were identified and the NDVI values of each AOI were fitted to an annual cycle model. In particular, as shown in Figs. 4(a), 4(b) and 4(c), the annual cycle models of AOIs #1 to #3 where forest fire occurred were changed. Moreover, while AOIs #4 to #5

Table 3. Changes in annual NDVI cycle models before and after forest fire in 2005

AOI		Change	Mean	Amplitude	Shift
Affected area	AOI #1	Before forest fire	0.4165	0.1668	0.9640
		After forest fire	0.3448	0.2420	0.8439
	AOI #2	Before forest fire	0.3817	0.1621	0.7641
		After forest fire	0.3011	0.2500	0.7267
	AOI #3	Before forest fire	0.3884	0.1620	0.7965
		After forest fire	0.3135	0.2361	0.7511
Nearby area	AOI #4	Before forest fire	0.4300	0.1701	0.8758
		After forest fire	0.4198	0.2178	0.8906
	AOI #5	Before forest fire	0.4110	0.1596	0.7869
		After forest fire	0.3935	0.2144	0.8500
Mountainous area	AOI #6	Before forest fire	0.4184	0.3087	0.9648
		After forest fire	0.4743	0.3012	1.1825
	AOI #7	Before forest fire	0.4311	0.3113	1.0424
		After forest fire	0.4578	0.3004	1.1090
	AOI #8	Before forest fire	0.4231	0.3210	0.9883
		After forest fire	0.4482	0.2935	1.1496
	AOI #9	Before forest fire	0.4441	0.2696	0.9773
		After forest fire	0.4771	0.2592	1.0935

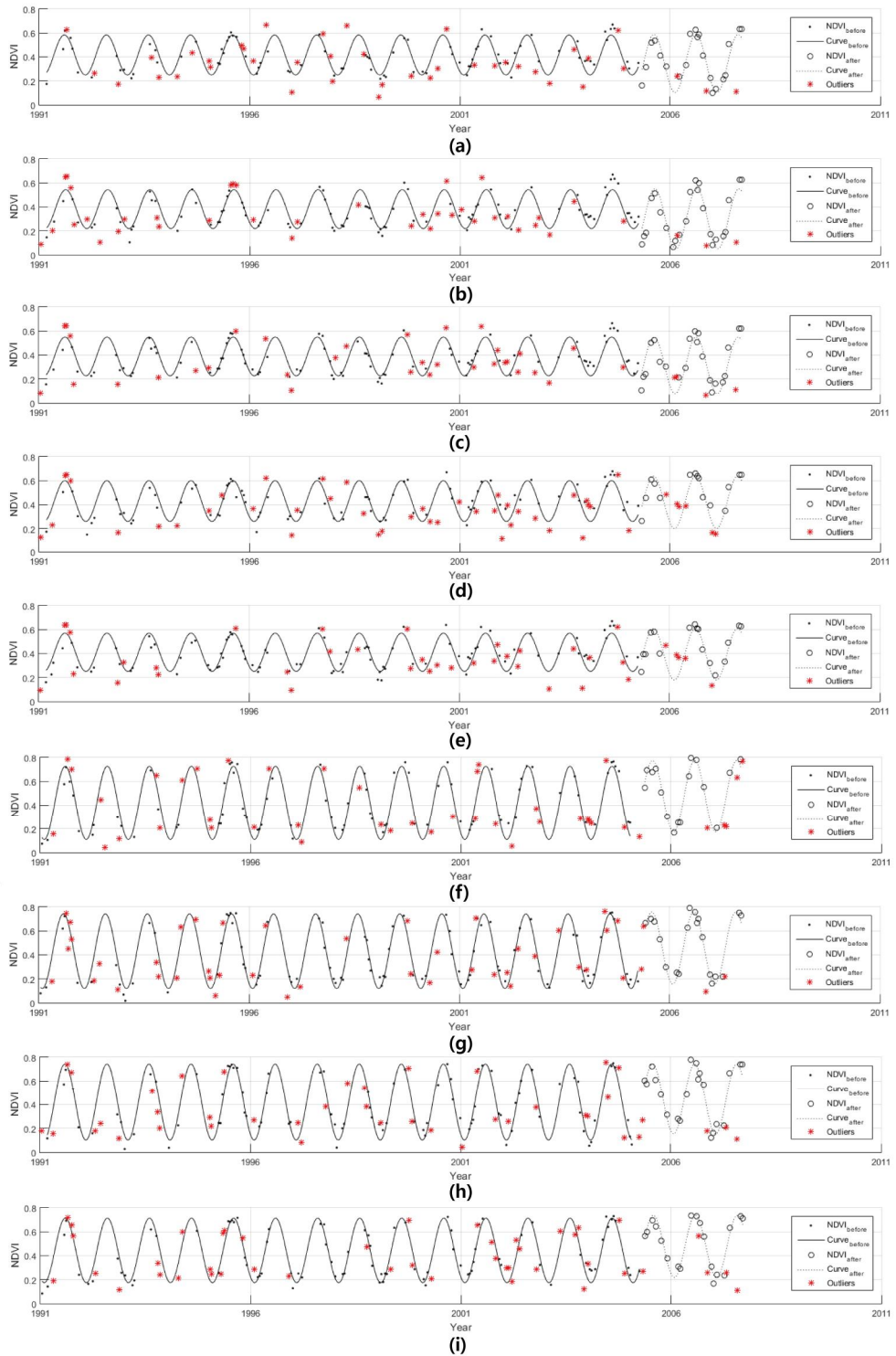


Figure 4. Annual NDVI cycle model of each AOI: (a) to (c) AOIs damaged by forest fire, (d) to (e) AOIs nearby forest fire-damaged areas, (f) to (i) AOIs in mountainous areas

Table 4. Changes of NDVI mean values before and after forest fire in 2005(analyzed images captured on 9 May 2003, 1 November 2003, 20 January 2004, 31 August 2004, 22 November 2005, 24 August 2007, 25 May 2009 and 5 February 2010)

AOI		Change	January 2004-2010	May 2003-2009	August 2004-2007	November 2003-2005
Affected area	AOI #1	Before forest fire	0.2777	0.4340	0.6310	0.3735
		After forest fire	0.2683	0.5424	0.6318	0.3203
	AOI #2	Before forest fire	0.2948	0.3578	0.6219	0.3541
		After forest fire	0.2118	0.4706	0.6078	0.2341
	AOI #3	Before forest fire	0.2510	0.3092	0.5231	0.3114
		After forest fire	0.2175	0.4132	0.5262	0.2627
Nearby area	AOI #4	Before forest fire	0.1501	0.1894	0.2611	0.1685
		After forest fire	0.1540	0.2227	0.2636	0.1869
	AOI #5	Before forest fire	0.1478	0.1740	0.2817	0.1711
		After forest fire	0.1681	0.2295	0.2846	0.1967
Mountainous area	AOI #6	Before forest fire	0.1130	0.4098	0.5975	0.2313
		After forest fire	0.2032	0.5959	0.6471	0.2440
	AOI #7	Before forest fire	0.0948	0.5202	0.6006	0.2302
		After forest fire	0.1825	0.6046	0.6474	0.1940
	AOI #8	Before forest fire	0.0524	0.3440	0.4240	0.1806
		After forest fire	0.1470	0.4115	0.3481	0.1585
	AOI #9	Before forest fire	0.2303	0.5924	0.6785	0.3833
		After forest fire	0.3236	0.6450	0.7092	0.3535

showed similar trends before and after the forest fire, the NDVI mean values in AOIs #1 to #3 dropped sharply about 0.07 after the forest fire. Meanwhile, NDVI mean values in AOIs #4 to #5 decreased about 0.02 and AOIs #7 to #9 increased about 0.03. The change of NDVI mean values in AOIs #4 to #5 displayed the insensible change but both areas showed a decreasing tendency. As both areas are the forest fire nearby area, it might be affected by the forest fire.

Amplitude of the annual NDVI cycle showed an increasing tendency of the forest fire-affected areas and nearby areas after the forest fire. In particular, the peak values of NDVI in Fig. 4 were stable even after forest fire. The reason why NDVI peak values were not much changed after the forest fire is that it might be influenced by reforestation program such as ‘Forest restoration plan at Yangyang special disaster district’ and ‘Forest management development project at major landscape area’(Korea Forest Service, 2013).

On the other hand, the NDVI trough values in Fig. 4 were distinctly decreased after the forest fire. It was because the NDVI trough values generally present vegetation condition in winter seasons and

the influence of the upper layer of trees is excluded. Therefore, the results demonstrated that the understory vegetation became bare soil after the forest fire.

At the mountainous areas, mean and amplitude values of the annual NDVI cycle are larger than those of the other areas. For AOIs #6 to #9, NDVI mean values increased by 0.02 and amplitude of annual cycle decreased by 0.01 after the forest fire. It is opposite trend with other areas, in which showed decreasing trend in mean values of NDVI and increasing trend in amplitude. The change of vegetation variability was insignificant and consistent tendency was observed.

On the other hand, the difference of the phase shift values before and after the forest fire was not significant because of the low spatial variability. The results implied that there was scanline error and time interval of the images was not too long to have influence on annual cycle model (Bechtel, 2012; Hong et al., 2015).

4.3 Single Imagery Analysis

To confirm the change tendency resulted from

NDVI annual cycle model, NDVI mean values of each AOIs compared with the results using a single image before and after the forest fire. It was difficult to get the available imagery to analyze annual and seasonal change of NDVI mean values before and after the event. Therefore, the images captured on 9 May 2003, 1 November 2003, 20 January 2004, 31 August 2004, 22 November 2005, 24 August 2007, 25 May 2009 and 5 February 2010 were analyzed. The results of analyzing with the imagery on January or February, May, August and November are listed on Table 4. The change tendency is similar to the results of NDVI annual cycle model. The NDVI mean values decreased on February and November and increased on May and August at the area affected by the forest fire. The effects in February and November are estimated because of the forest fire, and in May and August because of the influence of the reforestation program which performed after the event.

To detect the forest fire-damaged areas, single image analysis can be one of simple and reasonable solutions. However, it is difficult to obtain cloud-free data and analyze changes in annual trend. This is because each single image is captured in different time and environmental condition. The deficiency of data makes it difficult to decide whether the change is caused by the event or just affected by seasonal or climate change. In this regard, the NDVI annual cycle model using multi-temporal images can be useful to analyze overall tendency as well as change detection about specific event, because this model can simultaneously reflect seasonal effects and annual trend.

5. Conclusion

In this study, NDVI annual cycle model was proposed for vegetation analysis using Landsat images of Yangyang-gun, Gangwon-do. The time series of Landsat images before and after the forest fire on 2005 were used for validation of our algorithms.

Since the Landsat imagery might include noise pixels such as clouds and cloud shadows, Fmask and

RIRLS algorithms were applied to remove the noise pixels before applying annual cycle model. As a result of filtering, about 180 scenes of Landsat images among 285 scenes could be filtered and more stable modelling was conducted.

The NDVI annual cycle model could present the vegetation variability and the impact of the forest fire on vegetation. The mean values of NDVI in the forest fire-affected area were decreased by 0.07 and those in nearby area were dropped by 0.02. Accordingly, the amplitude of the NDVI annual cycle in the forest fire-affected area and nearby area had been increased after the forest fire. In particular, increase of trough values of the cycle models were higher than those of peak values. It implied that the understory vegetation was seriously damaged by the forest fire.

From the result of the experiment, it can be stated that NDVI annual cycle model is useful to monitor vegetation condition after a disastrous event. However, it is required for the analyzer to seriously consider quality, quantity and time period of data. In this sense, data of KOMPSAT 1, 2, 3 and 3A series which have very high spatial resolution and have been periodically collected can be a precious dataset and make valuable and precise research possible.

Acknowledgements

This research was supported by a grant [MPSS-IS-2014-111] through the Disaster and Safety Management Institute funded by Ministry of Public Safety and Security of Korean government.

References

1. Bechtel, B., 2012, Robustness of annual cycle parameters to characterize the urban thermal landscapes, *Geoscience and Remote Sensing Letters*, Vol. 9, No. 5, pp. 876–880.
2. Beck, P. S. A., Atzberger, C., Høgda, K. A., Johansen, B. and Skidmore, A. K., 2006, Improved monitoring of vegetation dynamics at very high latitudes: a new method using MODIS NDVI, *Remote Sensing of Environment*, Vol. 100, pp.

- 321–334.
3. Byun, S. W., 2014, Implementation of integrated systems for forest disaster management, *Korea Contents Association Review*, Vol. 12, No. 2, pp. 73–77.
 4. Chander, G. and Markham, B., 2003, Revised Landsat-5 TM radiometric calibration procedures and postcalibration dynamic ranges, *IEEE Transactions on Geoscience and Remote Sensing*, Vol. 41, No. 11, pp. 2674–2677.
 5. Ha, R., Shin, H. J. and Kim, S. J., 2007, Proposal of prediction technique for future vegetation information by climate change using satellite image, *Journal of the Korean Association of Geographic Information Studies*, Vol. 10, No. 3, pp. 58–69.
 6. Hatfield, J. L. and Prueger, J. H., 2015, Temperature extremes: effect on plant growth and development, *Weather and Climate Extremes*, Vol. 10, Part A, pp. 4–10.
 7. Hong, S. H., Cho, H. J., Kim, M. K. and Sohn, H. G., 2015, Analysis of urban heat island effect using time series of Landsat images and annual temperature cycle model, *Journal of the Korean Society for Geospatial Information System*, Vol. 23, No. 1, pp. 113–121.
 8. Jung, M. H. and Chang, E. M., 2013, Land-cover vegetation change detection based on harmonic analysis of MODIS NDVI time series data, *Korean Journal of Remote Sensing*, Vol. 29, No. 4, pp. 351–360.
 9. Korea Forest Service, 2013, Eco-forest restoration casebook, Korea Forest Service, <http://www.forest.go.kr>
 10. Labus, M. P., Nielsen, G. A., Lawrence, R. L., Engel, R. and Long, D. S., 2002, Wheat yield estimates using multi-temporal NDVI satellite imagery, *International Journal of Remote Sensing*, Vol. 23, No. 20, pp. 4169–4180.
 11. Lee, M. W., Lee, S. Y. and Lee, J. H., 2012, Study of the characteristics of forest fire based on statistics of forest fire in Korea, *Journal of Korea Society of Hazard Mitigation*, Vol. 12, No. 5, pp. 185–192.
 12. NASA, 2013, Landsat 7 science data users hand book, NASA, <http://landsathandbook.gsfc.nasa.gov/>
 13. O’Leary, D. P., 1990, Robust regression computation using iteratively reweighted least squares, *SIAM Journal on Matrix Analysis and Applications*, Vol. 11, No. 3, pp. 466–480.
 14. Street, J. O., Carroll, R. J. and Ruppert, D., 1988, A note on computing robust regression estimates via iteratively reweighted least squares, *The American Statistician*, Vol. 42, No. 2, pp. 152–154.
 15. Peters, A. J., Walter-Shea, E. A., Viña, A., Hayes, M. and Svoboda, M. D., 2002, Drought monitoring with NDVI-based standardized vegetation index, *Photogrammetric Engineering & Remote Sensing*, Vol. 68, No. 1, pp. 71–75.
 16. van Leeuwen, W. J. D., 2008, Monitoring the effects of forest restoration treatments on post-fire vegetation recovery with MODIS multitemporal data, *Sensors*, Vol. 8, No. 3, pp. 2017–2042.
 17. Verbesselt, J., Hyndman, R., Newnham, G. and Culvenor, D., 2010, Detecting trend and seasonal changes in satellite image time series, *Remote Sensing of Environment*, Vol. 114, pp. 106–115.
 18. Vermote, E. and Saleous, N., 2007, LEDAPS surface reflectance product description, Version 2.0, University of Maryland at College Park/Dept Geography and NASA/GSFC Code 614.5, <https://dwrgis.water.ca.gov/documents/269784/4654504/LEDAPS+Surface+Reflectance+Product+Description.pdf>
 19. Vila, J. P. S. and Barbosa, P., 2010, Post-fire vegetation regrowth detection in the Deiva Marina region(Liguria-Italy) using Landsat TM and ETM+ data, *Ecological Modelling*, Vol. 221, No. 1, pp. 75–84.
 20. Zhu, Z. and Woodcock, C. E., 2012, Object-based cloud and cloud shadow detection in Landsat imagery, *Remote Sensing of Environment*, Vol. 118, pp. 83–94.
 21. Zhu, Z. and Woodcock, C. E., 2014, Automated cloud, cloud shadow, and snow detection in multitemporal Landsat data: an algorithm designed specifically for monitoring land cover change, *Remote Sensing of Environment*, Vol. 152, pp. 217–234.
 22. Zhu, Z., Woodcock, C. E. and Olofsson, P., 2012, Continuous monitoring of forest disturbance using all available Landsat imagery, *Remote Sensing of Environment*, Vol. 122, pp. 75–91.